Electronic properties of single-walled silicon nanotubes compared to carbon nanotubes

Xiaobao Yang and Jun Ni

Department of Physics and Key Laboratory of Atomic and Molecular Nanoscience (Ministry of Education), Tsinghua University,
Beijing 100084, People's Republic of China
(Received 21 June 2005; published 22 November 2005)

Using the first principles method, we have investigated the electronic properties of Si-based single-walled nanotubes with different diameters and chiral vectors. The electronic properties show significant difference with those of carbon nanotubes. Si gearlike nanotubes (g-NTs) are more stable according to the formation energies, as Si atoms prefer the sp^3 hybridization. Si (n,n) $(n=5-11)$ g-NTs are semiconductors, whose gaps decrease as the diameters increase. Si $(n,0)$ $(n=10-24)$ g-NTs are semiconductors and the gaps decrease in a period of 3. The results for large Si g-NTs can be explained using the tight-binding model and the method of Brillouin zone foldings. The $(n,0)$ $(n=5-9)$ tubes are metal due to the σ^* and π^* mixing, which is rather strong for the small tubes.

I. INTRODUCTION

Carbon nanotubes have aroused scientific interest in various areas due to their great potential of applications.[1–6] The tubes have novel electronic properties attributed to their quasi-one-dimensional tubular structures, which can be metal or semiconductor depending on the diameters and chiralities.[1–3] Alkali atoms doping can enhance the conductivity of the bundles[4] and cause the metal-semiconductor transitions and semiconductor-semiconductor transitions.[5] Carbon nanotubes can also be the template of synthesizing SiC nanotubes via the chemical reactions.[6]

Silicon atoms have similar electronic configurations with carbon atoms. Theoretical and experimental research has been performed on Si clusters,[7] nanowires,[8] and tubular structures.[9–11] Si thin short nanowires are more stable than Si nanotubes built analogously as carbon nanotubes.[8] Quasi-one-dimensional structures can be stable, characterized by a core of bulklike fourfold-coordinated atoms surrounded by reconstructed surface structures with threefold-coordinated atoms.[10] Via the reaction of Si with carbon nanotubes, SiC nanotubes[6] have been synthesized, which shows a possible way of synthesizing Si nanotubes. Recently, silicon nanotubes are reported to be grown from silicon monoxide using the method of self-assembling.[13] It is shown that the individual Si nanotube has a hollow structure less than 4 nm in diameter and an interplanar spacing of 0.31 nm. The diffraction rings match well with the (111) and (220) diffraction rings of silicon. Si nanotubes can also be prepared by a CVD process using a nanochannel Al_2O_3 substrate[14] and porous alumina templates using molecular beam epitaxy.[15] Doping with $3d$ transition-metal atoms, finite silicon nanotubes can be stabilized, which indicates nanoscale magnetic device applications.[16]

The electronic properties of the possible Si nanotubes have been discussed by other authors.[9,11,12] Seifert *et al.*[11] showed that for Si nanotubes with additional electrons or H saturated, the gaps of $(n,0)$ tubes decrease to 2.50 eV as the diameter increases and the gaps of (n,n) tubes stay near 2.50 eV. Fagan *et al.*[9] claimed that Si hexagonal nanotubes

may exhibit metallic or semiconductor behaviors, similar to the corresponding carbon nanotubes. Zhang *et al.*[12] pointed out that gearlike structures should be the dominant form for Si nanotubes. The gaps of (n,n) tubes are inversely proportional to the diameters, which is in sharp contrast to the results from Fagan *et al.*[9]

In this paper, we compare the electronic properties and formation energies of Si hexagonal nanotubes (h-NTs) and gearlike nanotubes (g-NTs) with various of diameters and chirality. As shown in Fig. 1, Si h-NTs and g-NTs are formed by rolling the Si graphitelike sheet and the (111) sheet of diamond structure, respectively. The electronic properties of carbon nanotubes can be well explained using the tight-binding model and the method of Brillouin zone folding. Si h-NTs are built analogously as carbon nanotubes and the tight-binding model is almost the same, which shows the similar results from Fagan *et al.*[9] For Si g-NTs, we can use the modified model to give a good understanding of our results and Zhang *et al.*[9] from the first principles calculations. It should be emphasized that the difference in the electronic properties of Si g-NTs as compared to Si h-NTs is due to their lower symmetrical structures.

II. METHODS

We have performed the calculations of total energies and band structures of Si g-NTs and h-NTs using VASP (Vienna Ab initio Simulation Package).[17] The approach is based on an iterative solution of the Kohn-Sham equations of density functional theory in a plane wave basis set with Vanderbilt ultrasoft pseudopotentials.[18] We use the exchange correlation with the generalized gradient approximation given by Perdew and Wang.[19] We set the plane wave cutoff energy to be 200 eV. The Monkhorst-Pack scheme is used to sample the Brillouin zone.[20] The optimizations of the lattice constants and the atom coordinates are made by minimization of the total energy. The tolerance of energy convergence is 10^{-4} eV. All the structures are fully relaxed with a mesh of $1 \times 1 \times 9$ and the mesh of **k** space is increased to $1 \times 1 \times 20$ for the $(n,0)$ tubes and $1 \times 1 \times 40$ for the (n,n) tubes to
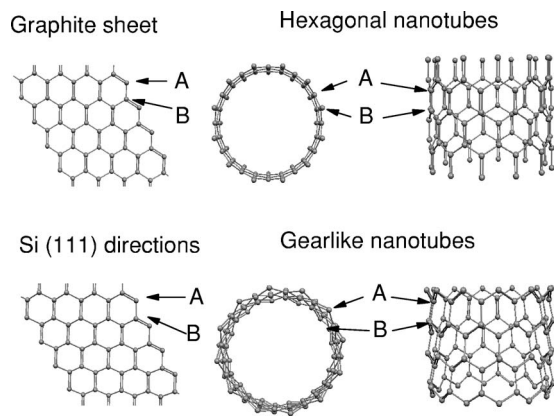
FIG. 1. Hexagonal nanotubes and gearlike nanotubes are formed by rolling the graphite and Si (111) sheets, respectively.

obtain accurate energies and band structures with atoms fixed after relaxations. We focus on the zigzag $(n,0)$ tubes and the armchair (n,n) tubes. The cell of these tubes contains $4n$ Si atoms. We have also chosen the supercells, which contain $8n$ and $12n$ Si atoms. In our calculations, no reconstructions occur for all the Si g-NTs and h-NTs.

III. RESULTS

Carbon nanotubes can be considered to be rolled from the graphite planar sheet, which is a triangular lattice with two inequivalent atoms. When rolled into nanotubes, two inequivalent atoms (A,B) have equal distance to the axis of the tube. As shown in Fig. 1, Si h-NTS are built in analogy with carbon nanotubes. For the Si bulk of the diamond structure, two inequivalent Si atoms are located in a triangular lattice in the (111) direction. However, the two lattices are not in a planar sheet. When Si g-NTs are formed by rolling the (111) sheet, two inequivalent Si atoms (A,B) have different distances to the axis of the tube. As shown in Fig. 2, the differences of formation energies per atom between Si g-NTs and h-NTs are 0.10 eV for the (3,3) tube and converge to 0.02 eV
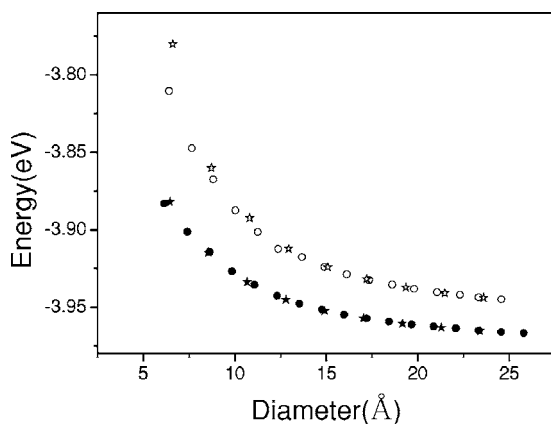

FIG. 2. Formation energies vs the diameters: circles for $(n,0)$ tubes and pentacles for (n,n) tubes, hollow ones for h-NTs and full ones for g-NTs, respectively. The formation energy of bulk diamond Si is −4.63 eV.
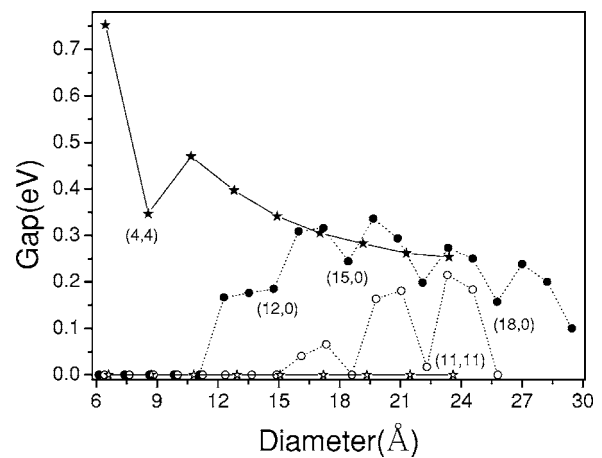

FIG. 3. Gaps vs the diameters: circles for $(n,0)$ tubes and pentacles for (n,n) tubes, hollow ones for h-NTs, and full ones for g-NTs, respectively.

for the (11,11) and (18,0) tubes. Thus, Si g-NTs are more stable than h-NTs, showing that the sp^3 hybridization is stable rather than the sp^2 hybridization, which is in agreement with the results from Zhang *et al.*[12] All structures are fully relaxed through the conjugate gradient method, with optimizations of both the lattice constants and the atom coordinates to minimize the total energies. Both the gearlike tubes and hexagonal tubes are chosen as the initial structures for relaxation. In our calculations, the gearlike and hexagonal tubes maintain their shape for little disturbance of atoms, which indicates these two kinds of structures are local optimized structures. However, the g-NTs are more stable when disturbed. For example, we consider the different initial structures of the (6,6) tube, using two triangular lattices with different distances to the axis. When the different distance is more than 0.04 Å, the tube would converge to the g-NTs, where the different distance to the axis of two triangular lattices is 0.5 Å. The total energies of Si g-NTs and h-NTs are obtained from the first principles calculations. The total energies are divided by the number of atoms to obtain the total energies per atom. The formation energies are obtained by subtracting the energy of a single isolated atom from the total energies per atom. The formation energies of Si g-NTs and h-NTs are about 0.7 eV higher than that of a Si diamond bulk structure (−4.63 eV). Zhang *et al.* performed the MD simulation on gearlike SiNTs at 500 K for 0.5 ps to test the stability of the calculated structures, finding that SiNTs with large diameters maintain the gearlike configurations.[12]

In the following, we focus on the electronic properties of Si h-NTs and g-NTs. We have performed calculations on the following Si NTs: the (n,n) tubes with $n \in (3,11)$ and the $(n,0)$ tubes with $n \in (5,24)$. Si (n,n) h-NTs with n varied from 3 to 11 are metal, which is in agreement with the results of Fagan *et al.*[9] In contrast, Si (n,n) g-NTs with n varied from 3 to 11 show that the gaps of the (n,n) tubes decrease as the diameters increase, as shown in Fig. 3. The local minima of the gaps occur at the (4,4) g-NTs. Our calculations show that Si $(n,0)$ h-NTs with n varied from 5 to 11 are metal. Fagan *et al.* have reported that the (10,0) h-NT is a semiconductor, however, with a very narrow gap.[9] Si $(n,0)$
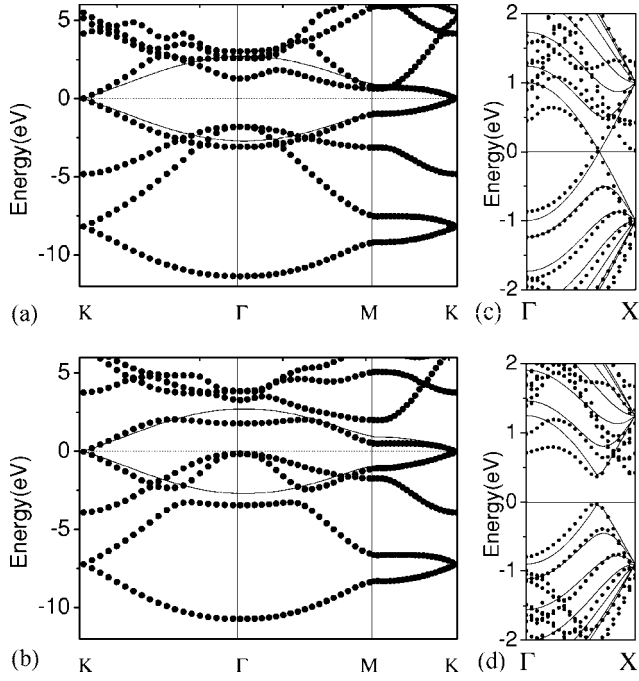
FIG. 4. Band structures: (a) the Si graphite sheet, (b) the Si (111) sheet, (c) (6,6) *h*-NTs, (d) (6,6) *g*-NTs. The dots are band structures obtained from the first principles calculations and the lines from the tight-binding methods.

h-NTs with *n* varied from 12 to 18, are metal when *n* = 12, 15, 18, which is in analogy with the results of carbon nanotubes.[1] However, for Si (*n*, 0) *g*-NTs with *n* varied from 12 to 24, are semiconductors and the gaps decrease in a period of 3, as shown in Fig. 3. When *n* = 15, 18, 24, the gap is the local minima. Si (*n*, 0) *g*-NTs with *n* varied from 5 to 9 are metal. As is known, the (*n*, *m*) carbon nanotubes are metal when $n - m = 3q$ (*q* is an integer).[1] Thus, we give the detailed comparisons of the (6,6) and (12,0) tubes, both *h*-NTs and *g*-NTs. For the (6,6) tube, the formation energy per Si atom for the *h*-NTs is 0.03 eV higher than the *g*-NTs. The diameter of the (6,6) *h*-NTs is 12.94 Å while the *g*-NTs have two kinds of diameters, 12.28 and 13.28 Å. As shown in Fig. 4(c), the *h*-NTs are metal with two bands degenerate at $k = 2\pi/(3a)$, which is in agreement with Fagan *et al.*[9] In contrast, the *g*-NTs have a gap of 396.6 meV at $k = 2\pi/(3a)$ shown in Fig. 4(d), which is in agreement with Zhang *et al.*[12] For the (12,0) tube, cohesive energy per Si atom for the *h*-NTs is 0.03 eV higher than the gearlike one. The diameter of the (12,0) *h*-NTs is 14.91 Å while the *g*-NTs have two kinds of diameters, 14.25 and 15.24 Å. As shown in Fig. 5(a), the (12,0) *h*-NT is metal and there are two bands degenerate at *k* = 0. In contrast, the (12,0) *g*-NT is a semiconductor with a gap of 185.2 meV at *k* = 0, as shown in Fig. 5(b).

The results above can be well explained under the tight-binding model, using the method of Brillouin zone foldings,[1,2] which have been used successfully to describe the gaps and band structures of carbon nanotubes. For the 2D graphene sheet, we construct two Bloch function form atomic orbitals for the two inequivalent carbon atoms (*A*, *B*), as shown in Fig. 1. Considering only nearest-neighbor inter-
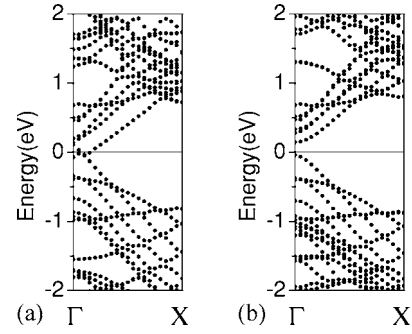

FIG. 5. Band structures: (a) (12,0) *h*-NTs and (b) (12,0) *g*-NTs.

actions, we obtain the eigenvalues $E(\mathbf{k})$ (Ref. 1) as a function $\omega(\mathbf{k})$, k_x, and k_y:

$$E_{g2D}(\mathbf{k}) = \frac{\varepsilon_{2p} \pm t\omega(\mathbf{k})}{1 \pm s\omega(\mathbf{k})}, \tag{1}$$

where ε_{2p}, *t*, and *s* are the orbital energy of the 2*p* level, the transfer integral, and the overlap integral between the nearest *A* and *B* atoms, respectively. The function $\omega(\mathbf{k})$ for the triangular lattice is[1]

$$\omega(\mathbf{k}) = \sqrt{|f(\mathbf{k})|^2} = \sqrt{1 + 4\cos\frac{\sqrt{3}k_x a}{2}\cos\frac{k_y a}{2} + 4\cos^2\frac{k_y a}{2}}, \tag{2}$$

where *a* is the length of the basis vector for the lattice. Two π bands are degenerate at the K points [$\omega(\mathbf{k})=0$] through which the Fermi energy passes. Thus, the 2D graphene sheet is metal. When the sheet is rolled into the nanotubes, k_x, k_y are not independent.[1] For the (*n*, *m*) tubes, if $n - m = 3q$ (*q* is an integer), $\omega(\mathbf{k})$ can be zero and the tube is metal. Otherwise, the tube is a semiconductor.[1] For graphite, two π bands are degenerate if and only if $\omega(\mathbf{k}) = 0$. This is supported by the experimental measurements[3] and the results from the first principles calculations.[2] For some tubes with small diameter, the case is different due to strong σ^* and π^* mixing,[21] where the tight-binding model is not suitable. We have calculated the two kinds of Si sheets. The optimized lattice constants are 3.85 Å for the Si graphite sheet and 3.75 Å for the Si (111) sheet. As shown in Figs. 4(a) and 4(b), both the Si graphite and the Si (111) sheets are metal. The dots are the band structures obtained from the first principles calculations and the lines are from the tight-binding methods. The tight-binding parameters $\varepsilon_{2p} = 0$ and $s = 0$, $t = -0.9$ eV are obtained by fitting the two π bands near the Fermi level. These two π bands play an important role in the electronic properties when the sheet is rolled into the tube, as shown in our results below. When the Si graphite sheet is rolled into Si *h*-NTs, the band structures can be explained using the Brillouin zone folding under the tight-binding model. The Si (111) sheet is metal, however, when it is rolled into Si *g*-NTs, ε_{2p} for the two inequivalent Si atoms is different. Thus, the tight-binding model should be modified, which leads to the result that the (6,6) *g*-NTs are semiconductors.
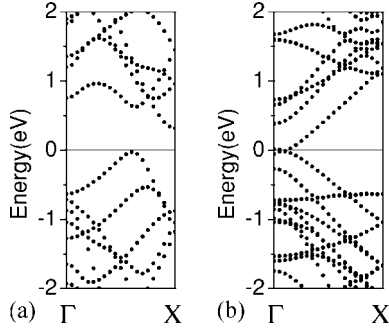
FIG. 6. Band structures: (a) (4,4) g-NTs and (b) (8,0) g-NTs.

For the case of Si nanotubes, when the hexagonal lattice is rolled into the nanotubes, the electronic properties of the Si nanotubes are similar to carbon nanotubes. As shown in Fig. 3, the (n,n) h-NTs are metal with two bands degenerate at $k=2\pi/(3a)$ through which the Fermi energy passes. As shown in Fig. 4(c), the (6,6) h-NTs are metal. We have also made the tight-binding calculations for comparison. The parameters of tight binding are $\varepsilon_{2p}=0$, $t=-0.9$ eV, and $s=0$, which is obtained by fitting the first principles calculations. The results of the tight-binding methods also show the (6,6) h-NTs are metal. The $(n,0)$ h-NTs with n varied from 12 to 18, are metal when $n=12,15,18$, which is in analogy with the results of carbon nanotubes.[1] However, for Si g-NTs, there are two kinds of triangular lattices in Si g-NTs, having different distances to the axis of the tube. For example, the (12,0) g-NTs have two kinds of diameters, 14.25 and 15.24 Å.

Thus, we obtained a Hamiltonian matrix with different diagonal elements

$$H_{AA} \neq H_{BB}. \qquad (3)$$

We use $H_{AA}=\varepsilon>0$ and take $H_{BB}=0$ as the zero point of the energy. The modified Hamiltonian matrix is

$$H = \begin{pmatrix} \varepsilon & tf(\mathbf{k}) \\ tf(\mathbf{k})^* & 0 \end{pmatrix}. \qquad (4)$$

Then the energy dispersion relations can be obtained

$$E[\omega(\mathbf{k})] = \frac{(\varepsilon - 2ts\omega^2) \pm \sqrt{\varepsilon^2 - 4ts\varepsilon\omega^2 + 4t^2\omega^2}}{2(1-s^2\omega^2)}. \qquad (5)$$

In general, the transfer integral t is minus. Thus, the eigenvalues would never be degenerate even if $\omega(\mathbf{k})=0$. For large tubes, we can use $s\cong 0$. Then $E_+-E_-=\sqrt{\varepsilon^2-4ts\varepsilon\omega^2+4t^2\omega^2}$ and E_+-E_- have a minima of ε when $\omega(\mathbf{k})=0$.

For (n,n) tubes, we have $n\sqrt{3}k_xa=2\pi m$, $m=1,2,\ldots,2n$. Thus, the energy dispersion relations can be obtained:[1]

$$E_m(k_y) = \pm t\sqrt{1 + 4\cos\frac{m\pi}{n}\cos\frac{k_ya}{2} + 4\cos^2\frac{k_ya}{2}},$$

$$-\frac{\pi}{a} < k_y < \frac{\pi}{a}. \qquad (6)$$

For $(n,0)$ tubes, we have $nk_ya=2\pi m$, $m=1,2,\ldots,2n$. Thus,

the energy dispersion relations can be obtained:[1]

$$E_m(k_x) = \pm t\sqrt{1 + 4\cos\frac{\sqrt{3}k_xa}{2}\cos\frac{m\pi}{n} + 4\cos^2\frac{m\pi}{n}},$$

$$-\frac{\pi}{\sqrt{3}a} < k_x < \frac{\pi}{\sqrt{3}a}. \qquad (7)$$

Thus, the gaps should occur at $k=2\pi/(3a)$ for the (n,n) tubes and at $k=0$ for the $(n,0)$ tubes, which is confirmed by our calculation results. As shown in Fig. 3, the gaps of (n,n) $[n\in(5,11)]$ g-NTs decrease as the diameters increase, because the difference between two triangular lattices becomes smaller and ε tends to be zero. As shown in Fig. 4(d), the (6,6) g-NTs are semiconductors. We have also made the tight-binding calculations for comparison. The parameters of tight binding are $\varepsilon=0.4$, $t=-0.9$ eV, and $s=0$, which are obtained by fitting the first principles calculations. The results of the tight-binding methods also show the (6,6) g-NTs are semiconductors. Si $(n,0)$ g-NTs with n varied from 15 to 24 are semiconductors and the gaps decrease in a period of 3, as shown in Fig. 3. When $n=15,18,24$, the gap is the local minima. All gaps occur at $k=0$, because E_+-E_- has a minima when $\omega(\mathbf{k})$ is taken as its minima. When n is the multiple of 3, $\omega(\mathbf{k})$ has a minima of zero and E_+-E_- has a minima of ε. The difference between two triangular lattices becomes smaller and ε tends to be zero. Thus, the gaps decrease in a period of 3.

In the following, we discuss the band structures of the tubes with small diameters. As shown in Fig. 3, the local minima of the gaps of the (n,n) g-NTs occur at (4,4). The $(n,0)$ g-NTs with n varied from 5 to 9 are metal. For those small tubes of (3,3) and (4,4), the gaps do not occur at $k=2\pi/(3a)$, which is due to the σ^* and π^* mixing, analogous as the case of carbon nanotubes.[21] The band structure of (4,4) g-NTs is shown in Fig. 6(a). For those small tubes of (5,0) $\sim(9,0)$, the gaps do not occur, due to the σ^* and π^* mixing. As an example, the band structure of (8,0) g-NTs is shown in Fig. 6(b).

IV. SUMMARY

In summary, we have shown that Si g-NTs have different electronic properties as compared to Si h-NTs and carbon nanotubes, according to our first principles calculations. Si g-NTs are more stable according to the formation energies, as Si atoms prefer the sp^3 hybridization. Si (n,n) $(n=5-11)$ g-NTs are semiconductors, whose gaps decrease as the diameters increase. Si $(n,0)$ $(n=10-24)$ g-NTs are semiconductors and the gaps decrease in a period of 3. Si (n,m) g-NTs with large diameters are semiconductors, whose gaps decrease with the increase of diameters and the local minima of gaps occur when $n-m$ is the multiple of 3. Si h-NTs have similar electronic properties with carbon nanotubes, which can be metal [for the (n,n) tubes] or semiconductors, depending on the diameters and chiralities. Under the tight-binding model and using the method of Brillouin zone fold-

ing, we have given reasonable explanations for the results. For Si g-NTs, there are two inequivalent triangular lattices whose distances to the axis are different. The asymmetry of the structures cause the (n,m) tubes to be semiconductors, even if $n-m$ is the multiple of 3, for which Si h-NTs and carbon nanotubes are metal.

[1] R. Saito, G. Dresselhaus, and M. S. Dresselhaus, *Physical Properties of Carbon Nanotubes* (Imperial College Press, London, 2003).

[2] N. Hamada, S. I. Sawada, and A. Oshiyama, Phys. Rev. Lett. **68**, 1579 (1992).

[3] J. W. G. Wildoer, L. C. Venema, A. G. Rinzler, R. E. Smalley, and C. Dekker, Nature (London) **391**, 59 (1998).

[4] R. S. Lee, H. J. Kim, J. E. Fischer, A. Thess, and R. E. Smalley, Nature (London) **388**, 255 (1997).

[5] X. Yang and J. Ni, Phys. Rev. B **71**, 165438 (2005).

[6] X. H. Sun, C. P. Li, W. K. Wong, N. B. Wong, C. S. Lee, S. T. Lee, and B. T. Teo, J. Am. Chem. Soc. **124**, 14464 (2002).

[7] T. Bachels and R. Schöfer, Chem. Phys. Lett. **324**, 365 (2000).

[8] B. X. Li, P. L. Cao, R. Q. Zhang, and S. T. Lee, Phys. Rev. B **65**, 125305 (2002).

[9] S. B. Fagan, R. J. Baierle, R. Mota, Antonio J. R. da Silva, and A. Fazzio, Phys. Rev. B **61**, 9994 (2000).

[10] M. Menon and E. Richter, Phys. Rev. Lett. **83**, 792 (1999).

[11] G. Seifert, T. Köhler, K. H. Urbassek, E. Hernandez, and T. Frauenheim, Phys. Rev. B **63**, 193409 (2001).

[12] R. Q. Zhang, H. L. Lee, W. K. Li, and B. K. Teo, J. Phys. Chem. B **109**, 8605 (2005).

[13] Y. W. Chen, Y. H. Tang, L. Z. Pei, and C. Guo, Adv. Mater. (Weinheim, Ger.) **17**, 564 (2005).

[14] J. Sha, J. J. Niu, X. Y. Ma, J. Xu, X. B. Zhang, Q. Yang, and D. Yang, Adv. Mater. (Weinheim, Ger.) **14**, 1219 (2002).

[15] S. Y. Jeong, J. Y. Kim, H. D. Yang, B. N. Yoon, S. H. Choi, H. K. Kang, C. W. Yang, and Y. H. Lee, Adv. Mater. (Weinheim, Ger.) **15**, 1172 (2003).

[16] A. K. Singh, T. M. Briere, V. Kumar, and Y. Kawazoe, Phys. Rev. Lett. **91**, 146802 (2003).

[17] G. Kresse and J. Hafner, Phys. Rev. B **47**, R558 (1993); **49**, 14251 (1994); G. Kresse and J. Furthmüller, Comput. Mater. Sci. **6**, 15 (1996); Phys. Rev. B **54**, 11169 (1996).

[18] D. Vanderbilt, Phys. Rev. B **41**, R7892 (1990).

[19] J. P. Perdew, J. A. Chevary, S. H. Vosko, K. A. Jackson, M. R. Pederson, D. J. Singh, and C. Fiolhais, Phys. Rev. B **46**, 6671 (1992).

[20] H. J. Monkhorst and J. D. Pack, Phys. Rev. B **13**, 5188 (1976).

[21] H. J. Liu and C. T. Chan, Phys. Rev. B **66**, 115416 (2002).